Interplay of defect cluster and the stability of xenon in uranium dioxide from density functional calculations

Hua Y. Geng,[1] Ying Chen,[2] Yasunori Kaneta,[2] Motoyasu Kinoshita,[3,4] and Q. Wu[1]
[1]*National Key Laboratory of Shock Wave and Detonation Physics, Institute of Fluid Physics, CAEP, P.O. Box 919-102, Mianyang, Sichuan 621900, People's Republic of China*
[2]*Department of Systems Innovation, The University of Tokyo, Hongo 7-3-1, Tokyo 113-8656, Japan*
[3]*Nuclear Technology Research Laboratory, Central Research Institute of Electric Power Industry, Tokyo 201-8511, Japan*
[4]*Japan Atomic Energy Agency, Ibaraki 319-1195, Japan*
(Received 21 March 2010; revised manuscript received 23 August 2010; published 14 September 2010)

Self-defect clusters in bulk matrix might affect the thermodynamic behavior of fission gases in nuclear fuel such as uranium dioxide. With first-principles local spin-density approximation plus U calculations and taking xenon as a prototype, we find that the influence of oxygen defect clusters on the thermodynamics of gas atoms is prominent, which increases the solution energy of xenon by a magnitude of 0.5 eV, about 43% of the energy difference between the two lowest lying states at 700 K. Calculation also reveals a thermodynamic competition between the uranium vacancy and trivacancy sites to incorporate xenon in hyperstoichiometric regime at high temperatures. The results show that in hypostoichiometric regime neutral trivacancy sites are the most favored position for diluted xenon gas, whereas in hyperstoichiometric condition they prefer to uranium vacancies even after taking oxygen self-defect clusters into account at low temperatures, which not only confirms previous studies but also extends the conclusion to more realistic fuel operating conditions. The observation that gas atoms are ionized to a charge state of Xe^{+} when at a uranium vacancy site due to strong Madelung potential implies that one can control temperature to tune the preferred site of gas atoms and then the bubble growth rate. A solution to the notorious metastable states difficulty that frequently encountered in density functional theory plus U applications, namely, the quasiannealing procedure, is also discussed.

DOI: 10.1103/PhysRevB.82.094106 PACS number(s): 61.72.J−, 71.15.Nc, 71.27.+a

I. INTRODUCTION

The thermodynamics of fission products in uranium dioxide has been a focus of considerable experimental and theoretical attentions in nuclear industry. Xenon as the most important fission gas is one of them. Concern has been particularly centered on xenon's role in fuel *swelling*—that could increase the pressure on the cladding of the fuel rod under irradiation and lead to rupture. A similar risk also exists for the container of nuclear waste in storage conditions. This has accordingly led to a desire to obtain a greater understanding of the basic processes governing the migration and trapping of xenon within the fuels.[1–5]

Previous theoretical studies on xenon behavior employed interatomic potentials such as shell model.[1–3] This method provided qualitative understanding of gas properties. However, since shell model has severe transferability difficulty,[6] the reliability of its results requires further verification by other methods. Application of quantum mechanics to this problem was available only recently and focused mainly on single gas atoms that occupying point vacancies and Schottky sites.[7–12] In uranium dioxide, however, oxygen defect clusters dominate and the interplay of them and fission gases might be the key to correctly understand the subtle material behavior. For example, in hyperstoichiometric regime of UO_{2+x}, where $x>0$, oxygen self-defect cluster—the cuboctahedron (COT) cluster dominates when temperature is relatively low.[13–17] There is a big cavity at the center of COT, which can either be empty (denoted as COT-v) or be filled by additional oxygen and forms COT-o cluster, or be filled by xenon atom and becomes COT-xe. Furthermore, existence of COT-v and COT-o clusters changes the concentrations of all other defect traps that the gas atoms can incorporate with. Such kind of direct and indirect effects of oxygen clusters have not yet been investigated. Big cavity also can be found at uranium vacancy or trivacancy (tri-V, a kind of bound Schottky). We will show that xenon atoms are prone to occupying these traps and become xenon-trap aggregates. This incorporation behavior not only reduces elastic strains that imposed on the bulk matrix but also changes the development of intragranular bubbles, and thus is possible to alleviate the fuel swelling that suffered from fission gases.

Energetics of xenon in defective UO_2 was modeled in a $2\times2\times2$ supercell consisting of eight fluorite cubic unit cells. Periodic boundary conditions and the density functional theory (DFT) in local spin-density approximation with Hubbard correction to the on-site Coulombic repulsion of the localized uranium $5f$ orbitals (LSDA+U) were employed to compute the total energy.[18–20] All structures were fully relaxed until residual forces less than 0.01 eV/Å. Details of the computational setup and the validation of the method are referred to Refs. 17, 21, and 22. Particularly the LSDA+U approach has been applied to perfect[23] and self-defective[17,21,22] UO_2 successfully, and yielded results in good agreement with experiments. Oxygen defect clustering and the relevant thermodynamics have also been well described by this method.[17,22]

In next section we will discuss a solution to the notorious metastable states problem that frequently encountered in DFT+U applications. This approach was developed in our previous calculations.[17,21,22] Though it lacks a rigorous theoretical basis and cannot guarantee that the true ground state

 ©2010 The American Physical Society

can always be achieved, we found that it is effective to reduce the frequency of encountering high-lying metastable states and thus improves the reliability of the computational results. In Secs. III and IV a systematic analysis of the electronic structure and energetics of xenon atoms that incorporating in nuclear fuels will be given, as well as the influence of oxygen defect clustering on the incorporation energies, the solution energies and the relevant thermodynamics of xenon gas. In Sec. V a comparison with other theoretical results will be discussed, followed by a summary.

II. QUASIANNEALING PROCEDURE

A. Theoretical argument

DFT+U formalism improves the performance of density functional theory on strongly *correlated* electronic system by including a Hubbard correction to the on-site Coulombic repulsion in a semiempirical manner. The cost is, however, introduced a lot of *local minima* on the energy surface that obstructing energy minimization process, and making electronic optimization algorithms get stuck in metastable states. Monitoring the occupation matrices (MOMs) of the localized f orbitals can solve this problem partially by varying their initial values to search for the lowest state.[24–26] But this option is not generally available in most DFT packages. Also the approach is a try and error method, which cannot ensure that the global minimum has already been obtained before all possible occupation matrices have been tried. Another concern about MOM is the computational cost. If spin degree is not considered, there are C_7^n different ways of filling n electrons in seven f levels diagonally. The number of different nondiagonal occupation matrices is much larger but we can reduce it to several times of the number of the diagonal case by assuming that all other occupations are insignificant. Thus for each atom there are mC_7^n different ways to fill the f levels, with m less than 10. It is also the total number of the runs that are required for each calculation if the simulation cell contains only one symmetry inequivalent atom. Unfortunately the symmetry of defective system is usually low, and has several nonequivalent atoms (say, k) with localized f electrons. In such a case a total number of $(mC_7^n)^k$ runs are necessary for each calculation. For UO_2, n equals 2 and m can take 3, thus gives about 60 different occupation matrices for each uranium.[25] If point defects are concerned, there are at least two nonequivalent uranium atoms, and the number of the total runs would increase to 3600. For defect clusters, k should be greater than 3 and it requires millions of runs for each calculation to get the final result. This is a huge burden even for modern supercomputers.

In a classical system, the metastable states difficulty can be tackled satisfactorily with *annealing* procedure. Namely, to remove the thermal kinetic energy of a system gradually and slowly so that all low-lying states have been visited before picking out the ground solution. Similar concept can be applied to electronic system. The basic idea is to shake or heat the electronic system with a spurious energy noise to help it overcome the energy barriers. We call this method the *quasiannealing* (QA) procedure.

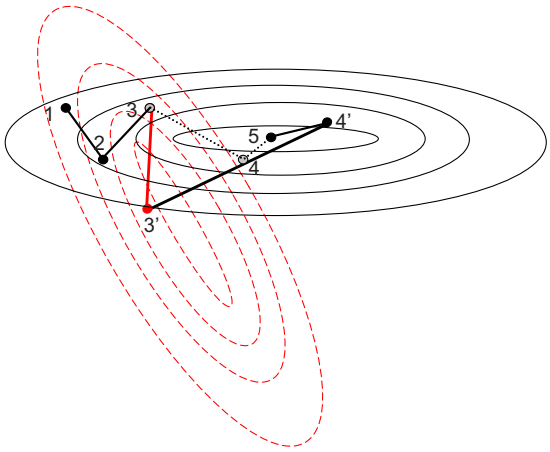

FIG. 1. (Color online) Schematic illustration of the electronic optimization process in quasiannealing procedure, where fluctuations of potential surface (here from the solid to the dashed and then back to the original solid contours) due to ionic drifts drag the minimizing path from 1, 2, 3, 4, 5 to 1, 2, 3, 3′, 4′, 5, thus circumvents possible metastable states on the original route.

The theoretical basis is that the electronic energy is a functional of the electron density $n(r)$, which is in turn a unique functional of the external potential $v(r)$. One can then convey the spurious noise from the ionic subsystem to the electronic subsystem via $v(r)$. It amounts to $\int \Delta v(r) n(r) dr$, where $\Delta v(r)$ is the fluctuation of the external potential. By switching off this spurious energy gradually, one can extract the ground state in a similar way as its classical counterpart. Alternatively, we can understand the mechanism of removal of the metastable states in QA procedure by tracking the electronic minimization process: the potential fluctuations alter the minimization path iteratively, thus being capable of avoiding any possible metastable states that lying on its route, as illustrated in Fig. 1.

In practice, one might exploit the *residual energy* of the minimization process. The energy uncertainty δE due to nonconvergence of the self-consistency field (SCF) gives a quasirandom fluctuation in ionic forces, which in turn leads to a Gaussian distribution of the ions with respect to their physical positions. The potential fluctuation Δv arising from this ionic drift eventually *heats* the electronic system up. Generation of Δv from the forces can be done with standard structure optimization algorithms. That is, one iteratively relaxes the ionic structure with an electronic state having a SCF tolerance of δE. In this realization, the only one parameter—the residual energy in SCF—controls the spurious noise in the electronic system. Its value should be large enough at the beginning so that the electronic system can travel freely in the phase space. By decreasing δE gradually, one converges the electronic system down to the ground state.

The merits of QA are not just that it can be used to tackle the metastable states. By coupling with ionic relaxation, one can optimize the electronic and ionic states simultaneously. It reduces the total computational cost dramatically when structure optimization is also required, especially when DFT+U formalism is employed where the SCF convergence is very slow. To avoid ions drifting too far away from the target

configuration, one needs to restore the structure after some ionic steps. Usually allowing cell volume and shape to vary improves the performance, because it not only extends the searching space, but also shakes the system globally and breaks the *symmetry* imposed by the Bravais lattice, which is one of the main reasons that lead to high-lying metastable states in strongly correlated system.[24,25]

B. Validation

The QA procedure is summed up as follows, where in each step the computation restarts from the wave function that was generated in its previous step:[27] (1) switch off symmetry, set appropriate values for SCF tolerance δE and ionic relaxation step size δr. (2) Employ standard ionic optimization algorithms to evolve the structure. (3) Reduce δE and δr slightly, restore the structure, go to step 2 and repeat the procedure until δE reaches the target precision. (4) Conduct a standard SCF iteration. (5) Slightly distort the structure, go to step 2 and repeat the whole process until no lower state can be found.

At first we discuss the performance of QA in a perfect fluorite cubic cell of PuO_2 (with 12 atoms) that ordering in 1**k** antiferromagnetic configuration with generalized gradient approximation (GGA)+U method. The projector augmented wave pseudopotentials and Perdew-Burke-Ernzerhof (PBE) exchange-correlation functional were used. The Hubbard parameters were 4.0 eV for U and 0.7 eV for J. A cutoff of 400 eV was adopted for the kinetic energy of the plane-wave basis, and 63 irreducible k points were used to sample the Brillouin zone. The lattice parameter was fixed at 5.45 Å. It should be pointed out that this setup was only for PuO_2. All the following defects calculations were conducted with LSDA+U method as detailed in Sec. I. Here we chose PuO_2 because this system has very stable metastable states. For example, if the cubic symmetry (O_h) is imposed onto the system, one always obtains a metastable state having a total energy of −125.282 eV, no matter what the initial condition of the calculation is. This is different from UO_2 where the symmetry-induced metastable state can be removed easily. In PuO_2, however, one has to switch off the symmetry in order to get rid of this state. As shown in Fig. 2, switching off the symmetry lowered the energy by 1.69 eV. But this is far from being the ground solution. Adiabatically switching on the Hubbard on-site interactions, namely, increasing the U and J parameters from zero slowly, further reduced the total energy about 0.16 eV. The QA procedure, in contrast, predicted a much lower energy. A total number of six independent QA runs were performed. The results were similar and the standard deviation σ (scattering of the data) was 0.006 eV. On the other hand, direct SCF calculations have a standard deviation of two orders larger than QA. This suggests that the electronic system has gotten rid of high-lying states and converged closely to the ground solution in QA. The best result we ever had is −127.684 eV.

It is helpful to compare QA results directly with MOM. We thus performed a GGA+U calculation on perfect UO_2 with the same setup as in Ref. 28. The only difference is that we used a 500 eV cut-off energy for the plane-wave basis set and a $5\times5\times5$ k-point mesh instead of the 600 eV cutoff and the $6\times6\times6$ k-point mesh that were used in that work. This difference should have little influence on the final result since the total energy has already been converged well with this setting of parameters. After a fully relaxation of the ionic structure, QA gave a total energy of −117.095 eV, lower than MOM's −116.505 eV for fluorite structure and −116.712 eV for Jahn-Teller distorted geometry (see Table V in Ref. 28). We cannot state that QA outperforms MOM but it is obvious that an incomplete implementation of MOM as done in Ref. 28 does not necessarily lead to a ground-state solution.

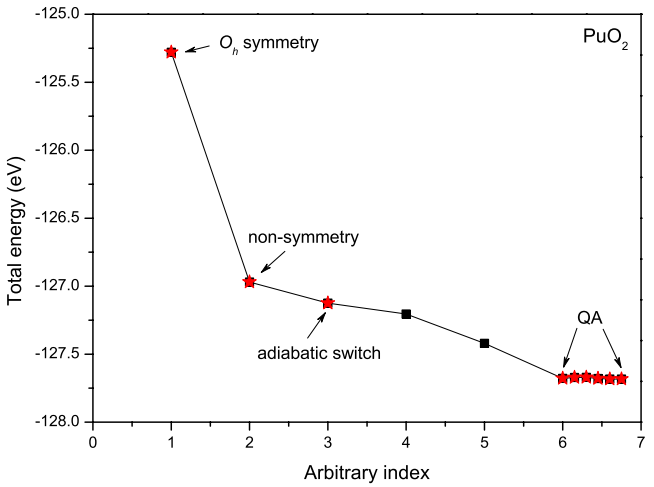

FIG. 2. (Color online) Main metastable states in PuO_2 and the performance of quasiannealing procedure, which predicted the lowest total energy.

Figure 3 demonstrates the improvement of QA procedure against direct SCF calculations for a set of defects in UO_2, including point oxygen interstitial, oxygen vacancy, uranium vacancy, split quad-interstitial, xenon atom that incorporated in a trivacancy site, and COT-o cluster. We found that direct

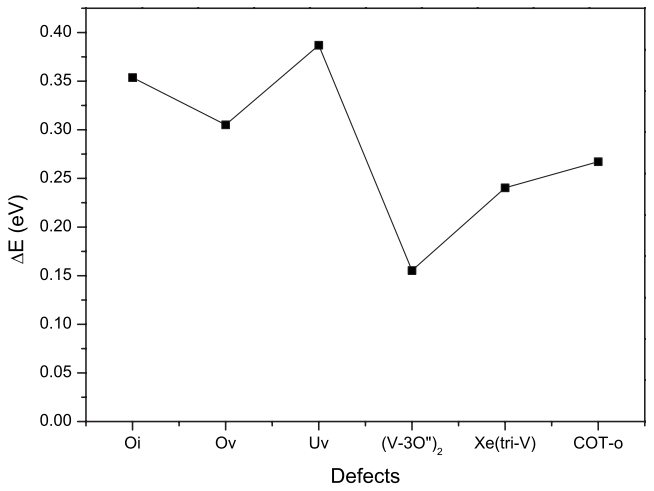

FIG. 3. Total-energy difference between direct SCF and QA calculations of some type of defects in UO_2, where the QA results are at the zero level. All direct SCF calculations were performed using the fully relaxed structures.

SCF calculations always stopped at high-energy states, with an energy distance about 0.3 eV to the QA results, regardless of the defect type. It is worthwhile to point out that these direct SCF calculations were performed on structures that already optimized by QA procedure, and the cubic symmetry of the lattice had been switched off. One interesting example is about the stability of oxygen defect clusters. Andersson *et al.*[29] did LSDA+U calculations on the stability of defect clusters in UO_2 without QA treatment. The results were controversial: they predicted that the split quad-interstitial $(V\text{-}3O'')_2$ had an energy lower than COT-o cluster. Here we denote the split quad-interstitial by the symbol $(V\text{-}3O'')_2$ because it is actually a linear combination of two basic clusters—$V\text{-}3O''$, an oxygen vacancy surrounded by three Willis O″ interstitials.[22] A careful recomputation of the energetics of these two clusters with QA procedure, however, gave a different picture. We found that Andersson *et al.*'s energy of $(V\text{-}3O'')_2$ was almost the same as QA. But their value of COT-o was much higher than that of QA (in terms of formation energy with respect to the same reference state, −10.38 eV vs −12.41 eV). A direct SCF run with QA-optimized structure led to a metastable state with an energy of 0.16 eV higher than that of QA and was much lower than Andersson *et al.*'s original result. A recheck calculation using the same setup as theirs also failed to reproduce their results. According to the variational principle of energy, we guess that their calculation of COT-o cluster might have stopped at a metastable state. Unfortunately we cannot identify it without reproducing their electronic state successfully.

Now we have two approaches that can tackle metastable states, i.e., MOM and QA. In the case of perfect UO_2, though primary MOM calculations did not predict a lower state than QA, it does not mean QA truly achieved the ground state. We know that annealing procedure does not perform well when there are a lot of local minima that have the same amplitude and the same width. Thus it cannot state that the metastable states problem has been solved satisfactorily by QA. However, QA is effective to remove high-lying metastable states and to bring the system down to one of the low-lying states that have small amplitude. From the experience of MOM,[25,26] we estimate the absolute error in QA might be less than 0.1 eV. The relative energy difference between systems would be much better and at an order of 2σ due to error cancellation. In practice, QA is an effective method to reduce data scattering and to improve the reliability of the calculated energetics.

In brief, when the system is small and the computer resource is enough so that allowing to repeat the calculation many times, MOM is a good choice. With this method one can get explicit information of how the metastable states distribute. On the other hand, QA optimizes ionic and electronic degrees simultaneously. Thus if atomic structure optimization is desired, QA would outperform MOM, especially for large systems. All of the following calculations have been treated by QA procedure to improve the reliability of the results.

III. FORMATION ENERGY AND INCORPORATION ENERGY

The formation energy of a defect D that has n excess oxygen atoms is defined as

$$E_D^f = E_D^{coh} - E_{per}^{coh} - \frac{n}{2}E_{O_2} \tag{1}$$

and for a defect with m excess uranium atoms is

$$E_D^f = E_D^{coh} - E_{per}^{coh} - mE_{\alpha U}. \tag{2}$$

Here the cohesive energy E_D^{coh} of a defective structure is calculated from its total energy by subtracting the isolated spin-polarized atomic contributions and E_{per}^{coh} is the cohesive energy of the corresponding structure without defect; E_{O_2} is the binding energy of a neutral dioxygen molecule; and $E_{\alpha U}$ is the cohesive energy per atom in the metallic α-U phase.[21] For trivacancy that keeps the UO_2 composition unchanged, the formation energy is given by

$$E_{tri}^f = E_{tri}^{coh} - \frac{N-1}{N}E_{per}^{coh}, \tag{3}$$

where N is the total number of UO_2 formula that contained in the perfect cell. The incorporation energy of xenon is defined by

$$E^i = E_{Xe(X)}^{total} - E_X^{total} - E_{Xe}, \tag{4}$$

where $E_{Xe(X)}^{total}$ is the total energy of a cell in which the xenon atom is at the trap site X, E_X^{total} is the total energy of the same cell containing only the trap X, and E_{Xe} is the total energy of an isolated xenon atom. If taking xenon-trap aggregate as a single defect complex, one can define its formation energy similar to Eq. (1) or Eq. (2) except that here E_{Xe} also should be deducted. Numerically it is equal to the sum of the trap formation energy and the incorporation energy of xenon at that trap.

The calculated results of structure and energetics of various trap sites and xenon-trap aggregates in UO_2 are listed in Table I. The tri-V is a kind of bound Schottky defect that has the same geometry as shown in Fig. 3(e) of Ref. 1, i.e., a pair of oxygen vacancies that binding with one of its nearest uranium vacancies. It is believed that this geometry has the lowest energy.[1,11] Defects $V\text{-}4O''$, $V\text{-}3O''$, and $(V\text{-}3O'')_2$ are not included here.[22] The trap in these clusters is too small to accommodate xenon atoms: introducing one xenon atom completely destroys the trap geometry and the aggregate becomes unstable. In addition, previous investigations showed that these defects have insignificant concentration comparing with others.[17,22]

The energetic information in Table I is interpreted as for isolated defects. This is appropriate for point defects since the simulation cell is large enough for them. But for extensive clusters such as COT, the cell is not large enough and the interactions with their images that arising from the periodic boundary conditions might be remarkable, with dipole-dipole interactions as the leading contribution. Therefore the obtained energy is more close to the value of an ordered configuration of the clusters at the corresponding concentration. Using this energy to describe diluted clusters is theoretically questionable. But the quality will become better and better as the concentration gets increasing. Fortunately, COT clusters only appear in the hyperstoichiometric regime and

TABLE I. LSDA+U results for structural and energetic properties of defects in uranium dioxide: defect traps [the trivacancy (tri-V), the octahedral interstitial site (Int.), the uranium site (U), and the oxygen site (O)] and xenon-trap aggregates [COT-xe—xenon in COT cluster and Xe(X)—Xe in trap X], respectively. ΔV is the defect-induced volume change that averaged to per fluorite cubic cell (over eight cells totally). E^f is the formation energy, E^i is the incorporation energy, and q is the Bader effective charge of xenon. The data of three oxygen self-defects are also included for reference, see Ref. 17 for details.

	COT-xe	Xe(Int.)	Xe(U)	Xe(O)	Xe(tri-V)	tri-V	COT-v	COT-o	O_i (Int.)
ΔV (Å^3)	0.79	3.74	0.97	3.99	1.40	0.54	−0.14	−1.61	−0.29
E^f (eV)	−4.08	9.75	12.92	15.06	5.17	4.99	−7.18	−12.41	−2.17
E^i (eV)	3.10	9.75	3.87	7.53	0.18				
$q(\|e\|)$	0.20	0.26	0.96	0.14	0.09				

have high enough concentrations,[17] which implies that the size effects of COT clusters might have little impact on our discussion here.

COT-xe has the lowest formation energy (as defined above) in all of the defects considered here, followed by Xe(tri-V), Xe(Int.), Xe(U), and Xe(O). The high formation energy of Xe(U) is due to the contribution of the uranium vacancy trap, whereas the low value of COT-xe is because of the excess oxygen atoms, with each one contributing about −2 eV. Thus it is helpful to divide the xenon-trap aggregate formation energy into two parts: the trap formation energy and the energy that is required to incorporate xenon atom into the pre-existing trap. The latter is called incorporation energy and is also listed in Table I. We see that the most easy trap for xenon to incorporate with is trivacancy, followed by COT cluster and uranium vacancy.

It is understandable that rare gases such as xenon and krypton need a big *space* for them to be accommodated in the fuel matrix, and gas-fuel incorporation is usually accompanied with drastic swelling of the latter, especially when the gas atoms occupy mainly the octahedral sites [Xe(Int.)] or oxygen vacancies [Xe(O)]. But if most of the gas atoms go into pre-existing traps that have comparable size, for example, uranium vacancies, trivacancies, or COT clusters, the resulting fuel deformation will be much small, as can be perceived from the ΔV row of Table I. This primary analysis indicates that xenon prefers to COT clusters or uranium vacancies instead of octahedral sites or oxygen vacancies. From Table I we can see that the incorporation energy is as high as 9.75 eV (7.53 eV) when xenon is at an octahedral site (oxygen vacancy), and decreases to 3.1 eV when goes into COT cluster. This suggests that there is a deep local minimum on the energy surface at COT center, which will drive xenon atoms from octahedral sites and oxygen vacancies into COT clusters. Similar conclusion holds for trivacancy and uranium vacancy.

Figure 4 illustrates in details how this takes place in UO_2, where the energy variation for different combinations of xenon atom and excess oxygen atoms is given. For clarity we assumed here that point xenon occupies an octahedral site. The discussion is similar if it is at an oxygen vacancy. Point oxygen interstitials are also assumed occupying octahedral sites. In Fig. 4(B) the competition between COT-v and COT-o clusters is demonstrated. The energy cost is about 1.5 eV to bring four-point oxygen interstitials together to form a COT-v cluster. The energy gain is 6.5 eV when the xenon atom goes into COT-v center from an octahedral site. Most of this part of energy gain is from the *elastic* contribution. Similarly, swapping the central oxygen of COT-o with a xenon atom reduces the total energy by 3.5 eV. The preference of xenon to COT trap is thus evident in both cases. It is easy to understand this by size effects: the atomic size of xenon is larger than the octahedral site, thus a drastic lattice distortion occurs when xenon atom occupying an octahedral site. But it is not when xenon is in COT clusters. Therefore as long as there are COT-o or COT-v clusters, xenon atoms will combine with them instead of occupying octahedral sites or oxygen vacancies.

Note that there are two kinds of incorporation process for COT-xe: (a) a direct combination of a xenon atom and a pre-existing COT-v cluster; and (b) swap a xenon atom with the central oxygen of a COT-o cluster. In the first case the total xenon-trap aggregate formation energy is −4.08 eV, with a xenon incorporation energy of 3.10 eV, and a trap formation energy (COT-v) of −7.18 eV, as listed in Table I. In the latter case, however, the total formation energy is −6.25 eV (with −2.17 eV contributed by the point oxygen interstitial), with the xenon incorporation energy of 6.16 eV, and the trap formation energy (COT-o) of −12.41 eV. Therefore in the case (a) the incorporation is easy but the available number of COT-v trap is rare, whereas in the case (b) the situation is just opposite.

To understand this kind of incorporation behavior, the mechanism of the energy variation from COT-o to COT-v is

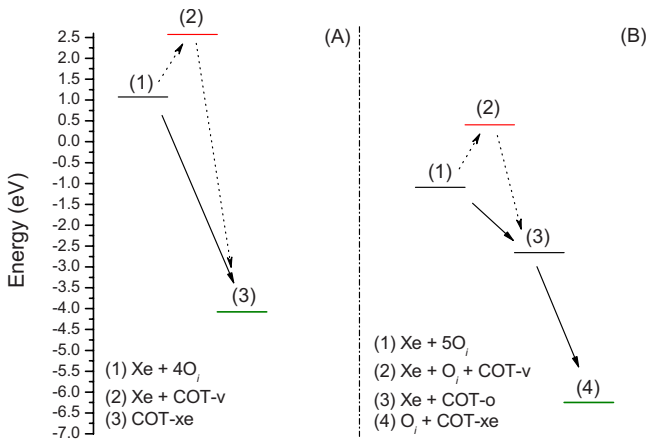

FIG. 4. (Color online) Formation energy of various defect arrangements in UO_2: (a) a system with one xenon atom and four excess oxygen atoms, and (b) with one more excess oxygen.

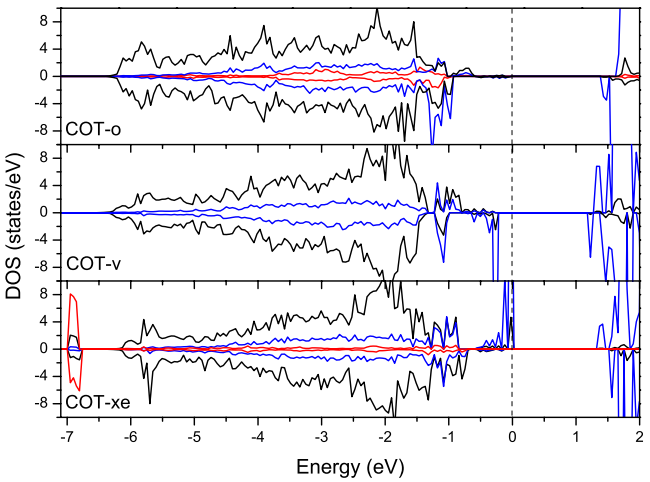

FIG. 5. (Color online) Density of states of O $2p$ (black) and U $5f$ (blue, or dark gray in print version) orbitals that projected onto the defect atoms in COT-o (upper panel), COT-v (middle panel), and COT-xe (lower panel), respectively. Contribution from the central atom (oxygen in COT-o and xenon in COT-xe) is marked by red (light gray in print version) lines. The dotted vertical line indicates the Fermi level.

the key. Figure 5 shows the electronic density of state (DOS) of oxygen $2p$ and uranium $5f$ orbitals that projected onto the cuboctahedron atoms of COT-o, COT-v, and COT-xe, respectively. The red (light gray i print version) lines indicate the contribution from the oxygen or xenon atom that occupies the cluster center, and the dotted vertical line indicates the Fermi level. There are three significant features: (1) the distribution profile of the O $2p$ DOS within the main valence band, (2) the localized U $5f$ states just below the Fermi level, and (3) the interplay of the localized xenon state and the valence band.

In COT-o, the central oxygen not only hybridizes itself with U $5f$ states directly but also enhances the overlapping of the main O $2p$ and U $5f$ orbitals near the upper band edge. As a result, the localized U $5f$ states just below the Fermi level are absorbed into the valence band. This makes COT-o stable in energetics. In contrast, in COT-v and COT-xe, the hybridization with localized U $5f$ states is insufficient. Though a weak antibond is formed by partial overlapping, a highly localized state still presents near the Fermi level. This feature and the fact that O $2p$ DOS distributes more on the upper part in the main valence band reveal the electronic origination of the energy increase from COT-o to COT-v. Different from oxygen whose effect is at the upper band edge, xenon in COT-xe affects mainly the lower edge of the valence band. As shown in the lower panel of Fig. 5, xenon interacts with itinerant O $2p$ and U $5f$ orbitals weakly, splitting the main valence band into a minor localized bonding state and a major antibonding band that is dispersive. The latter is then pushed to higher energy and is the main contribution to the energy difference between COT-xe and COT-v. Since this band shift keeps most features of the valence band unchanged, xenon effects on energetics are thus mainly mechanical.

Table I also lists the Bader effective charge of xenon in various traps at the last row.[30] We see that except trivacancy in which xenon is charge neutral, all other traps have a tendency to *ionize* xenon atom. Usually the degree of this ionization is small when the gas atom is in COT cluster, oxygen vacancy, or octahedral site. This is because of the relatively electron-rich environment of these traps. But in the case of Xe(U), one electron has been completely peeled off due to the strong Madelung potential of the periodic lattice at the uranium vacancy sites. It is a competition process between the electron affinity of the trap and the ionization energy of the gas atom. Thus the ionization does not lead to a large energy increase. The observed ionization of Xe to Xe^+ confirms Grimes and Catlow's[1] prediction with shell model. This charge transfer has important implication on gas bubble growth rate. It is believed that gas bubble grows by accumulation of point xenon impurities via diffusion. Positively charged gas atoms expel each other strongly due to the electrostatic interactions. Thus they cannot approach together. This means that inert gas bubble cannot initiate from uranium vacancies. In agreement with shell-model results, we found that fission gas bubbles can only start from neutral trivacancy sites.[2] As will be discussed below, this property makes temperature and the chemical composition being effective parameters to tune the growth rate of bubbles.

IV. SOLUTION ENERGY AT FINITE TEMPERATURES

With only the information of formation energy and incorporation energy that discussed in the previous section, it is difficult to evaluate what kind of trap the gas atoms prefer to at finite temperatures. For example, COT-xe has the lowest trap formation energy—which suggests a high concentration of the trap—but the incorporation energy is high. Thus it is not necessarily the favored one because the preferred site should be a combination result of the available number of the trap sites and the degree of incorporation difficulty. We knew from previous investigations on oxygen clustering behavior in UO_2 that in hypostoichiometric regime (UO_{2-x}) oxygen vacancy is the major defect,[21] and in UO_{2+x} there is a transition from point oxygen interstitials to COT-o clusters with an increase in the composition.[17,22] That is, oxygen vacancy and COT-o are the most available traps in UO_2. On the other hand, the concentrations of COT-v, uranium vacancy, and trivacancy are one order smaller but they have lower incorporation energies. Therefore a delicate analysis is required in order to get the final answer.

Theoretically, the probability for a gas atom to be trapped in a specific site is proportional to the product of the trap concentration ρ_t and the probability to incorporate the gas atom into one of these traps. In this way one can define the *solution energy* as

$$E^s = -\kappa_B T \ln \rho_t + E^i, \tag{5}$$

which gives the probability of trapping one gas atom to a specific trap by $\exp(-E^s/\kappa_B T)$. Here κ_B is the Boltzmann constant and T is the temperature. The first term in Eq. (5) gives the effective formation free energy of the trap and the second term is the incorporation energy. With independent cluster approximation,[17,21,22,31,32] one can evaluate the trap concentration as a function of temperature and chemical

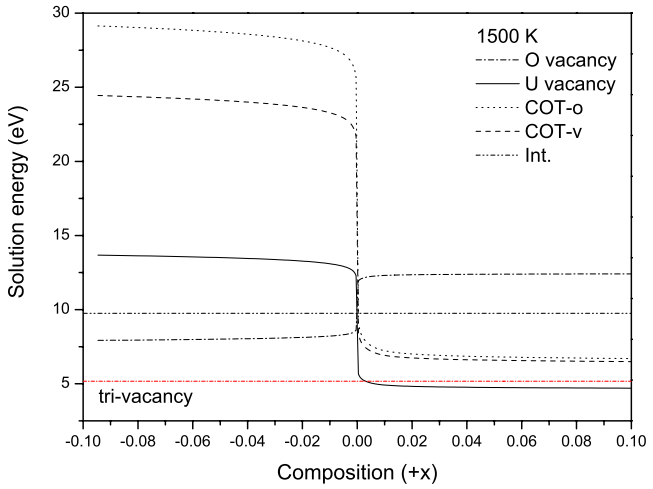

FIG. 6. (Color online) Solution energy of xenon at various traps in UO_2 at 1500 K.

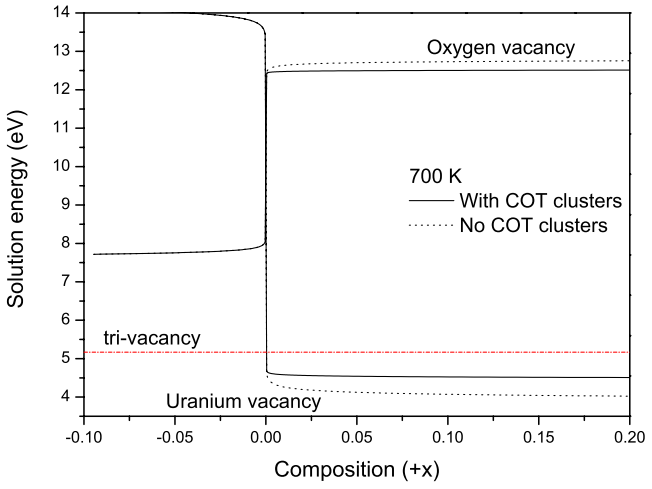

FIG. 7. (Color online) Influence of oxygen defect clustering on solution energy of xenon at 700 K.

composition in the closed regime. This approximation holds valid as long as there has no explicit *overlapping* or strong interactions among traps. Note that the temperature effect considered here is only the statistical effect on trap concentrations. Contribution from lattice vibrations on defect formation energy can be included straightforwardly but here we did not take this into account because we focus mainly on the fundamental incorporation behavior of single gas atoms.

Calculated solution energies of xenon at various trap sites at 1500 K are shown in Fig. 6. For trivacancy and octahedral interstitial sites, the solution energies are independent of composition since creation of these traps does not change the stoichiometry. The stoichiometric effects on oxygen vacancy and uranium vacancy are opposite. There is a steplike jump near the stoichiometry. Far away from that composition, the variation in solution energy flats out. In hypostoichiometric regime, trivacancy has the lowest solution energy. All other traps have a solution energy at least 3 eV higher, and the physical picture is clear and trivial. In the other side of the stoichiometry, however, thermodynamic competition becomes important. The solution energy of xenon at trivacancy sites is 5.15 eV. The solution energy for xenon at uranium vacancy sites is about 4.7 eV, slightly lower than that at trivacancy. This is different from shell-model results which predicted that cation vacancy had a much lower solution energy than trivacancy.[1] With LSDA+U calculations, though uranium vacancy has the lowest solution energy, the trivacancy is at a level of *just* 0.4 eV higher. In contrast, COT clusters are about 1.8 eV higher in solution energy, mainly due to the few concentration of COT-v trap in the incorporation process (a) and the great incorporation energy in the case (b).

When decrease the temperature to 700 K, because of the change in trap concentrations, the solution energy of xenon at uranium vacancy sites reduces 0.7 eV, as shown in Fig. 7. This change is important since it almost excludes the possibility for xenon atoms to occupy trivacancy sites. The influence of oxygen clusters is also nontrivial here. At 700 K, inclusion of COT clusters increases the solution energy of xenon at uranium vacancy sites by a value of 0.5 eV. This effect takes 43% of the solution energy difference between xenon at uranium vacancy and at trivacancy sites, thus is significant.[33] Furthermore, since concentration of oxygen defect clusters are inversely proportional to temperature,[17,22] at lower temperatures this indirect influence will become more distinct.

For all trap sites that were investigated in this work, the solution energies are positive. It indicates the insolubility of xenon gas in bulk UO_2. But as a fission reaction product, xenon keeps in the fuel matrix until it diffuses to grain boundaries and forms large bubbles. Before that, gas atoms might distribute randomly in the material and grow into small bubbles at defect sites or on dislocation loops. The moderate solution energy difference of xenon between at uranium vacancy and at trivacancy sites in $x>0$ regime suggests that one can change temperature to *tune* the incorporation behavior of xenon, and then the bubble growth rate.[34,35] This provides an alternative point to investigate the fuel swelling mechanism and the consequent structure damage imposed to the fuel and/or the cladding.

V. COMPARISON WITH OTHER THEORETICAL CALCULATIONS

There were several DFT calculations on the incorporation behavior of xenon in UO_2 published recently.[9,11,12] It is valuable to summarize these results and compare with our calculations. The results of DFT calculations and those computed using semiempirical shell-model potentials[1,3] are listed in Table II. These data are scattered but a common trend is obvious. All calculations that conducted at different theoretical levels predicted that the lowest incorporation energy for xenon is at the trivacancy site, and the highest energy is at the octahedral interstitial site, which is then followed by the oxygen and the uranium vacancy sites. Only the GGA results of Ref. 9 predicted a different order. Its Xe(U) has an incorporation energy as high as 13.9 eV. This might originate from size effect since they employed a small supercell containing only 12 atoms. In a recent GGA calculation using a

TABLE II. Calculated incorporation energies of xenon in UO_2 at various trap sites by different methods: the uranium site (U), the oxygen site (O), the octahedral interstitial site (Int.), the trivacancy site (tri-V), and the cuboctahedron site (COT).

E^i (eV)	COT-xe	Xe(Int.)	Xe(U)	Xe(O)	Xe(tri-V)
LSDA+U [a]	3.10	9.75	3.87	7.53	0.18
GGA+U [b]		11.11	2.5	9.5	1.38
GGA+U [c]		8.07	5.18	9.01	2.90
GGA[b]		12.75	6.04	9.71	2.12
GGA[d]		11.2	13.9	9.4	
Shell model[e]		17.23	4.99	13.34	1.16
Shell model[f]		18.67	5.83	15.15	3.3

[a]This work.
[b]Reference 11.
[c]Reference 12.
[d]Reference 9.
[e]Reference 1.
[f]Reference 3.

larger supercell containing 96 atoms,[11] this value was reduced to 6.04 eV and became qualitatively consistent with other calculations. In addition, there is a digital scattering with a magnitude of 1–2 eV in these DFT results. This might be due to the different methodologies that were employed, for example, the different exchange-correlation functionals, the constraints on structure optimization process, the effective Hubbard parameters, and so on. Metastable states might also play some role here.

The incorporation energies of xenon calculated by Nerikar *et al.*[11] are 1–2 eV higher than ours, except that at uranium vacancy where their value is about 1 eV smaller. As for the solution energies, they predicted the stability of xenon at trivacancy in the hypostoichiometric regime with a solution energy of 3.88 eV, about 2 eV smaller than ours. This is because though we have a similar binding energy for point defects to form a trivacancy, our formation energies of individual point defects are higher than theirs. In hyperstoichiometric regime, they and we both predicted that uranium vacancy is the favored site for xenon at low temperatures. Again our value is about 2 eV higher. Without considering oxygen clustering and finite temperature effects, Nerikar *et al.* failed to notice the variation in the solution energy with temperature and the thermodynamic competition among trivacancy, uranium vacancy, and other possible complex traps (e.g., divacancy), which we have shown are important for understanding the physical behavior of realistic nuclear fuels.

VI. CONCLUSION

With LSDA+U calculations, the incorporation behavior of xenon atoms at various trap sites in UO_2 was analyzed by studying the electronic structure and energetics. In the regime of UO_{2-x}, the result was that the gas atom prefers to trivacancy sites while in UO_{2+x} uranium vacancies are favored. COT clusters have large enough space at their centers but are not occupied by xenon atom due to subtle electronic dehybridization of O $2p$ and U $5f$ orbitals when xenon atom goes in and the central oxygen out. The calculated solution energies showed that a thermodynamic competition between Xe(U) and Xe(tri-V) is significant, and the indirect influence of oxygen clustering is important. At uranium vacancy site, xenon is ionized to Xe^+ state, confirmed early semiempirical prediction. This kind of charge transfer indicates that xenon bubbles cannot initiate from uranium vacancies but neutral trivacancy sites. Thus one can tune the occupation probability of xenon at trivacancy sites and then the bubble growth rate by control temperature. An approach to solve the metastable states difficulty that frequently encountered in DFT+U applications was proposed, which exploits the coupling between ionic and electronic subsystems and uses a quasiannealing procedure to relax the electronic system to the ground state. It was shown that this method can effectively avoid metastable states.

ACKNOWLEDGMENTS

Support from the Fund of National Key Laboratory of Shock Wave and Detonation Physics of China (Grant No. 9140C6703031004) is acknowledged. The work was also partially supported by the Budget for Nuclear Research of the Ministry of Education, Culture, Sports, Science and Technology of Japan (MEXT), based on the screening and counseling by the Atomic Energy Commission, and by the Next Generation Supercomputing Project, Nano-science Program, MEXT, Japan.

[1] R. W. Grimes and C. R. A. Catlow, Philos. Trans. R. Soc. London, Ser. A **335**, 609 (1991).
[2] R. A. Jackson and C. R. A. Catlow, J. Nucl. Mater. **127**, 167 (1985).
[3] S. Nicoll, Hj. Matzke, and C. R. A. Catlow, J. Nucl. Mater. **226**, 51 (1995).
[4] P. W. Winter and D. A. Macinnes, J. Nucl. Mater. **114**, 7 (1983); P. Blair, A. Romano, Ch. Hellwig, and R. Chawla, *ibid.* **350**, 232 (2006).
[5] J. Noirot, L. Desgranges, and J. Lamontagne, J. Nucl. Mater. **372**, 318 (2008).
[6] H. Y. Geng, Y. Chen, Y. Kaneta, and M. Kinoshita, J. Alloys Compd. **457**, 465 (2008).
[7] J. P. Crocombette, J. Nucl. Mater. **305**, 29 (2002).
[8] M. Iwasawa, Y. Chen, Y. Kaneta, T. Ohnuma, H. Y. Geng, and M. Kinoshita, Mater. Trans. **47**, 2651 (2006).
[9] M. Freyss, N. Vergnet, and T. Petit, J. Nucl. Mater. **352**, 144 (2006).
[10] P. Nerikar, T. Watanabe, J. S. Tulenko, S. R. Phillpot, and S. B. Sinnott, J. Nucl. Mater. **384**, 61 (2009).
[11] P. V. Nerikar, X. Y. Liu, B. P. Uberuaga, C. R. Stanek, S. R. Phillpot, and S. B. Sinnott, J. Phys.: Condens. Matter **21**, 435602 (2009).
[12] J. Yu, R. Devanathan, and W. J. Weber, J. Phys.: Condens. Matter **21**, 435401 (2009).
[13] D. J. M. Bevan, I. E. Grey, and B. T. M. Willis, J. Solid State Chem. **61**, 1 (1986).
[14] R. I. Cooper and B. T. M. Willis, Acta Crystallogr., Sect. A: Found. Crystallogr. **60**, 322 (2004).
[15] F. Garrido, R. M. Ibberson, L. Nowicki, and B. T. M. Willis, J. Nucl. Mater. **322**, 87 (2003).
[16] L. Nowicki, F. Garrido, A. Turos, and L. Thome, J. Phys. Chem. Solids **61**, 1789 (2000).
[17] H. Y. Geng, Y. Chen, Y. Kaneta, and M. Kinoshita, Phys. Rev. B **77**, 180101(R) (2008).
[18] G. Kresse and J. Furthmüller, Phys. Rev. B **54**, 11169 (1996).
[19] V. I. Anisimov, J. Zaanen, and O. K. Andersen, Phys. Rev. B **44**, 943 (1991).
[20] V. I. Anisimov, I. V. Solovyev, M. A. Korotin, M. T. Czyzyk, and G. A. Sawatzky, Phys. Rev. B **48**, 16929 (1993).
[21] H. Y. Geng, Y. Chen, Y. Kaneta, M. Iwasawa, T. Ohnuma, and M. Kinoshita, Phys. Rev. B **77**, 104120 (2008).
[22] H. Y. Geng, Y. Chen, Y. Kaneta, and M. Kinoshita, Appl. Phys. Lett. **93**, 201903 (2008).
[23] H. Y. Geng, Y. Chen, Y. Kaneta, and M. Kinoshita, Phys. Rev. B **75**, 054111 (2007).
[24] P. Larson, W. R. L. Lambrecht, A. Chantis, and M. van Schilfgaarde, Phys. Rev. B **75**, 045114 (2007).
[25] B. Dorado, B. Amadon, M. Freyss, and M. Bertolus, Phys. Rev. B **79**, 235125 (2009).
[26] G. Jomard, B. Amadon, F. Bottin, and M. Torrent, Phys. Rev. B **78**, 075125 (2008).
[27] A successful QA calculation requires to decrease the spurious energy slowly enough. It is a little tricky and needs some caution. Generally, one can simply check the sensitivity of the total energy with respect to the computational initial conditions to see whether the QA has been conducted properly or not, for example, the electronic optimization algorithms, the number of k points and the total bands that involved, the random number generator that used to generate the initial wave function, and so on.
[28] B. Dorado, G. Jomard, M. Freyss, and M. Bertolus, Phys. Rev. B **82**, 035114 (2010).
[29] D. A. Andersson, J. Lezama, B. P. Uberuaga, C. Deo, and S. D. Conradson, Phys. Rev. B **79**, 024110 (2009).
[30] G. Henkelman, A. Arnaldsson, and H. Jonsson, Comput. Mater. Sci. **36**, 354 (2006).
[31] Hj. Matzke, J. Chem. Soc., Faraday Trans. 2 **83**, 1121 (1987).
[32] A. B. Lidiard, J. Nucl. Mater. **19**, 106 (1966).
[33] The importance of oxygen clustering on thermodynamic bahavior of UO_2 also manifests in facilitating oxygen diffusion by via V-3O″ clusters, as discussed in D. A. Andersson, T. Watanabe, C. Deo, and B. P. Uberuaga, Phys. Rev. B **80**, 060101(R) (2009). Though in equilibrium states this cluster has a low concentration (see Ref. 22), they might present transiently as an intermediate state in the diffusion process of point oxygen interstitials.
[34] Temperature also affects the diffusivity of defects and micro gas bubbles, which in turn determines the development rate of grain-boundary bubbles.
[35] G. Sattonnay, L. Vincent, F. Garrido, and L. Thome, J. Nucl. Mater. **355**, 131 (2006).